

## HOLOGRAPHIC ARRAY FOR DETERMINING STRUCTURAL ACOUSTIC PROPERTIES

Jit Sarkar<sup>a</sup>, Sandrine T. Rakotonarivo<sup>a,b</sup>, Simone Sternini<sup>a</sup>, Alexis Bottero<sup>a</sup>, Earl G. Williams<sup>c</sup>, Jeffrey Dwayne Tippmann<sup>a,d</sup>, and William A. Kuperman<sup>a</sup>

<sup>a</sup>Scripps Institution of Oceanography, University of California, San Diego, 9500 Gilman Drive, La Jolla, California 92093-0238,

<sup>b</sup>Aix Marseille Univ, CNRS, Centrale Marseille, LMA UMR 7031, Marseille, France

<sup>c</sup>Naval Research Laboratory, Acoustics Division, Washington, DC 20375, USA

<sup>d</sup>Los Alamos National Laboratory, Intelligence and Space Research Division, P.O. Box 1663, Los Alamos, New Mexico 87545, USA

Contact author: William A. Kuperman

Scripps Institution of Oceanography, University of California, San Diego,

9500 Gilman Drive, La Jolla, California 92093-0238

wkuperman@ucsd.edu

**Abstract:** *It has already been shown that the scattering properties of an arbitrary object in an external medium can be determined by three quantities: The structural impedance matrix,  $Z_s$ , the input impedance matrix  $Z_i$ , and the radiation impedance matrix,  $Z_r$ . Only  $Z_s$  is dependent on the specific, possibly unknown and complicated internal structure of the object; the other two are only dependent on the surface shape of the object and the external medium so they can be routinely computed. We have constructed a laboratory facility to measure the structural impedance of an object by placing it in an external, diffuse noise field. The measurements are made using an array of a double layer of MEMS microphones placed in the near field of the object; the array is embedded in a skeletal structure which surrounds the object. This array structure is programmatically generated from a 3D scan of the object, and constructed using a large 3D printer. Cross correlating the MEMS acoustic data together with holographic signal processing yields the structural impedance, with the large matrix-matrix calculations being accelerated on a GPU computing platform. These results combined with the other computed impedances provides the scattering properties of the object when placed (loaded) in an external medium. The details of the experimental setup are explained and preliminary results are presented.*

**Keywords:** *Structural Acoustic , Holographic Array, Impedance Matrix, MEMS microphone array*

## INTRODUCTION

We have developed a method based on earlier work of Bobrovnikskii [1] to measure the in vacuo structural impedance (or admittance) matrix of a complex object by placing it in a random noise field and correlating pressures and velocities on its surface [2]. The importance of this procedure is that once the structural impedance matrix of an object is known, it can be combined with easily computable interior and exterior (radiation) impedances [1] that only depend on the object shape and the external medium. Furthermore, these impedances can be easily modified to determine the scattering properties of the object arbitrarily oriented in any medium [3–5], as opposed to intensive numerical modeling and/or exhaustive scattering experiments involved with measurements *in situ*. The components of the total theory [1,2] are illustrated in Fig.1 for which only  $Z_s$  need to be measured while the other two impedances are readily computed.

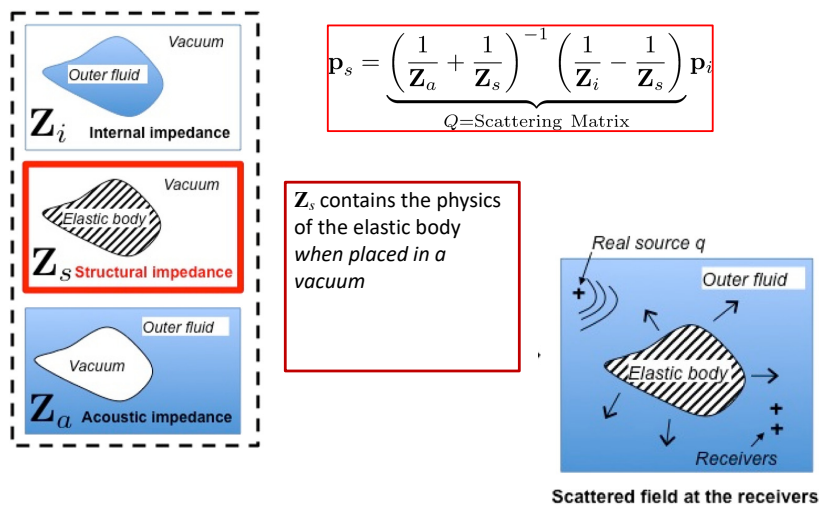


Figure 1: The scattered field is derived from three impedances

An experiment on an air-filled, thick spherical shell was carried out to demonstrate the measurement of the in vacuo structural admittance [6] using a small set of surface mounted accelerometers and microphones with remotely placed loudspeakers for excitation.

We are now constructing a laboratory facility which combines dual surface Nearfield Acoustical Holography (NAH) [7,8], Equivalent Source Method (ESM) [3,9] with Field Separation Techniques (FST) [10,11] for measuring the structural impedance of an object by placing it in an external, diffuse noise field. The measurements are made using an array of a double layer of Micro-Electro-Mechanical Systems (MEMS) microphones placed in the near field of the object; the array is embedded in a skeletal structure which surrounds the object. This array structure is programmatically generated from a 3D scan of the object, and constructed using a large 3D printer. Cross correlating the MEMS acoustic data together with holographic signal processing yields the structural impedance, with the large matrix-matrix calculations being accelerated on a Graphical Processing Unit (GPU) computing platform. These results combined with the other computed impedances (internal and acoustic) provide the scattering properties of the object when placed (loaded) in an external medium. The details of the experimental setup are explained and preliminary results are presented.

## 2. BACKGROUND THEORY FOR MEASUREMENT

The structural impedance is the ratio of the force and normal velocity at the surface of the object and as derived in [1,2] can be written in terms of matrices of the correlations of the surface pressures between (N) points on the surface and correlation of pressures and normal velocities between the same points on the surface as shown in Fig. 2, where  $\mathbf{p}$  and  $\mathbf{v}$  are vectors whose elements are the frequency domain pressures and normal velocities and the brackets denote an ensemble average over many (L) noise realizations.

**After ensemble averaging:**

$$\langle \mathbf{p} \mathbf{p}^H \rangle = -\mathbf{Z}_s \langle \mathbf{v} \mathbf{p}^H \rangle$$

**All are  $N \times N$  matrices**

**If sufficient number of spatially random realizations, we can invert** :  $\langle \mathbf{v} \mathbf{p}^H \rangle$

$$\mathbf{Z}_s = -\langle \mathbf{p} \mathbf{p}^H \rangle \langle \mathbf{v} \mathbf{p}^H \rangle^{-1}$$

**L realizations  
(random noise sources)**

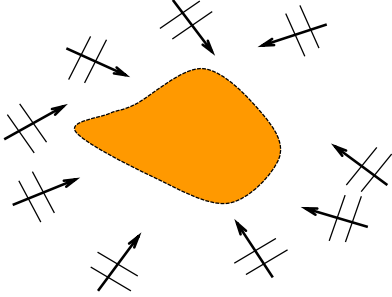


Figure 2: The structural impedance is derived from correlating surface pressures and normal velocities.

Our earlier measurements were of a spherical shell, such that its symmetry allowed using only a limited number of sensors on the surface [6]. An arbitrary shaped object required more intensive sensing so that a large number of sensors attached to the surface become problematic. To overcome this impediment, we employ NAH that utilizes sensors arranged on two concentric surfaces a small distance from the object [12] and then translate these measurements to surface pressure and normal velocity on the surface using FST together with ESM and subsequently implementing the process of Fig. 2 from which the scattered field can be obtained as per Fig. 1.

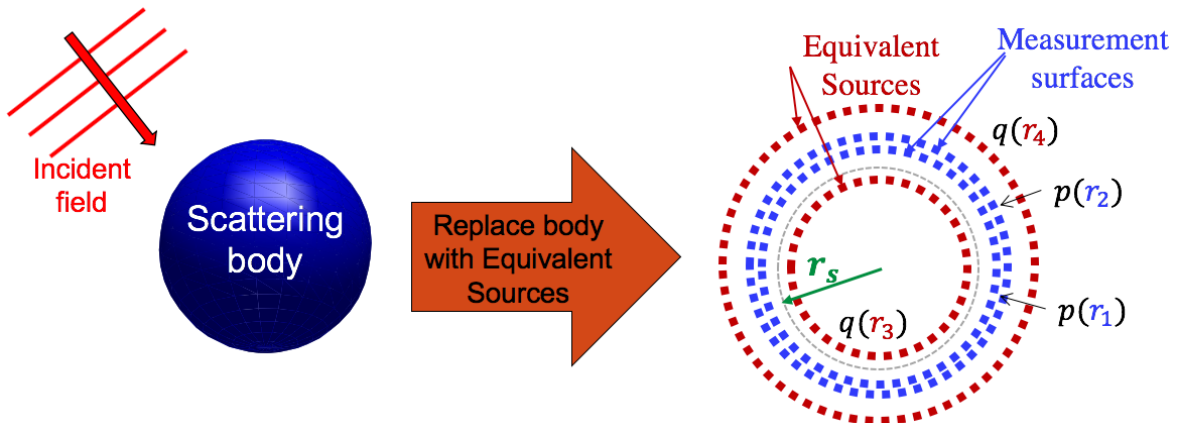


Figure 3: Combining ESM with FST: Data from two measurement layers of sensors,  $p(r_1)$  and  $p(r_2)$ , are used to construct two equivalent source arrays such that the  $q(r_3)$  sources and  $q(r_4)$  sources respectively separate scattered and incident fields which can then be propagated to the surface,  $r_s$ , of the object.

Referring to Fig. 3. the two layers of sensors,  $\mathbf{p}(\mathbf{r}_1)$  and  $\mathbf{p}(\mathbf{r}_2)$ , allow separation of incoming and scattered fields creating synthetic, surrogate source arrays (ESM) inside,  $\mathbf{q}(\mathbf{r}_3)$ , and outside,  $\mathbf{q}(\mathbf{r}_4)$ , the surface such that the scattered field is determined by the former and the incoming by the latter [10,11]. With that field separation, NAH can then determine the pressure and velocity at the object surface,  $\mathbf{r}_s$ . Free field Green's functions are used between the real sensors and equivalent source locations.

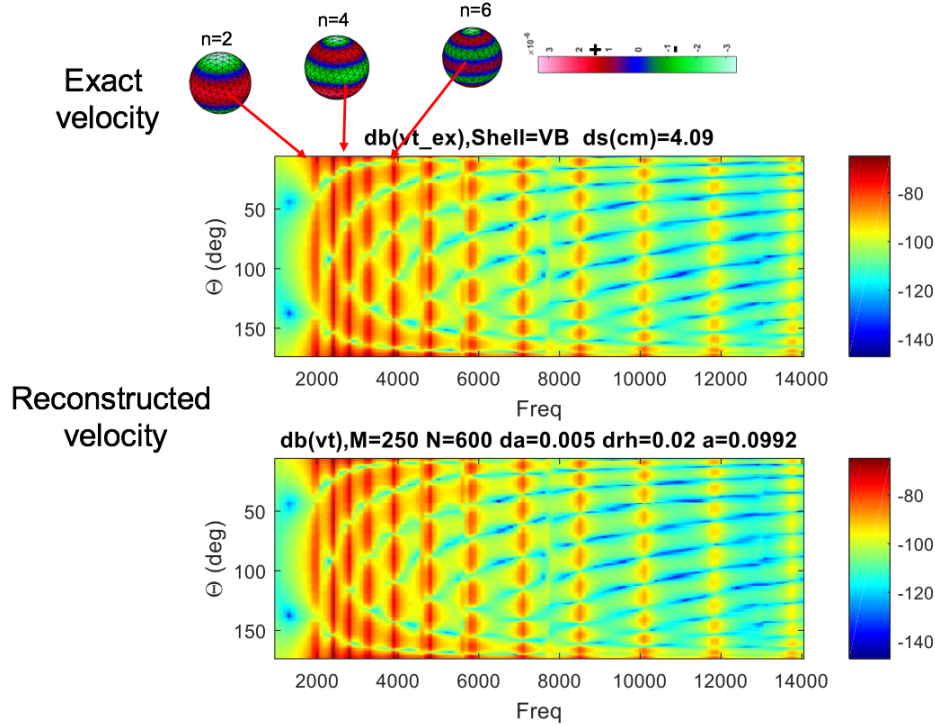


Figure 4: Comparison of a data analysis procedure based on the methodology of Figure 3 with an exact solution.

An example of the accuracy of the method is shown in Fig. 4 which compares a simulation involving the steps outlined in Fig. 3 for two layers of 250 pressure sensors separated by .5 cm with the inner layer being 2.0 cm from the sphere and 600 “Equivalent Sources” with an analytic result from which some of the shell modes are also shown.

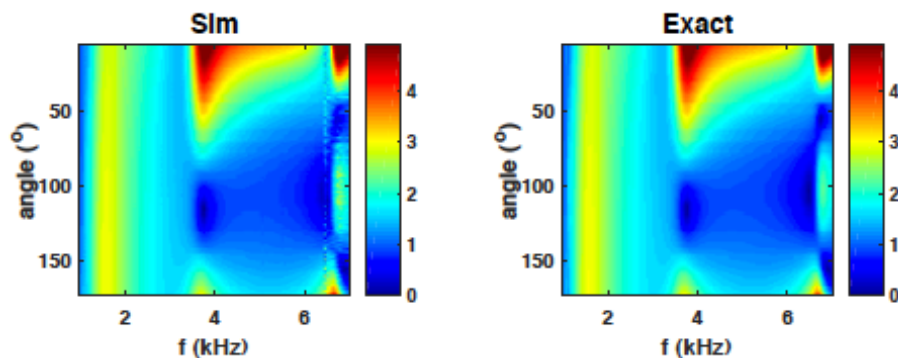


Figure 5: Comparison of Monte Carlo simulation of the holographic array processing with an analytic solution for scattering of a plane wave incident on a spherical shell.

Figure 5 then shows a comparison of a scattered field result in a water medium for a specific incident angle obtained by simulating the whole procedure as summarized by Figs. 1-3 with an

exact analytic solution. That is, as per Fig.1 the scattering matrix is a function of the three impedances. The simulation for computing  $Z_s$  involved a Monte Carlo simulation of the procedure illustrated in Fig. 2; the internal medium was the shell structure and to emulate a laboratory experiment, the external medium was air. (We had previously shown that this procedure to determine  $Z_s$  actually produced the required *in vacuo* result [2]). The other two impedances are easily computed using the external shape of the object and the acoustical properties of water for the “outer fluid” for  $Z_i$  and  $Z_a$ , thereby verifying that measurements from the holographic laboratory procedure could be translated to a water loaded scattering result.

### 3. CONSTRUCTING THE LABORATORY FACILITY

The actual facility to obtain the measurements simulated in the previous section requires several components operating in conjunction to provide the complete system.

A skeletal scaffold is designed around the target dimensions, to which pairs of sensors will be mounted in close proximity to the objects surface (support for ~250 planned). This support structure is fabricated on a large form-factor 3D printer, providing the flexibility to accommodate targets of almost any shape.

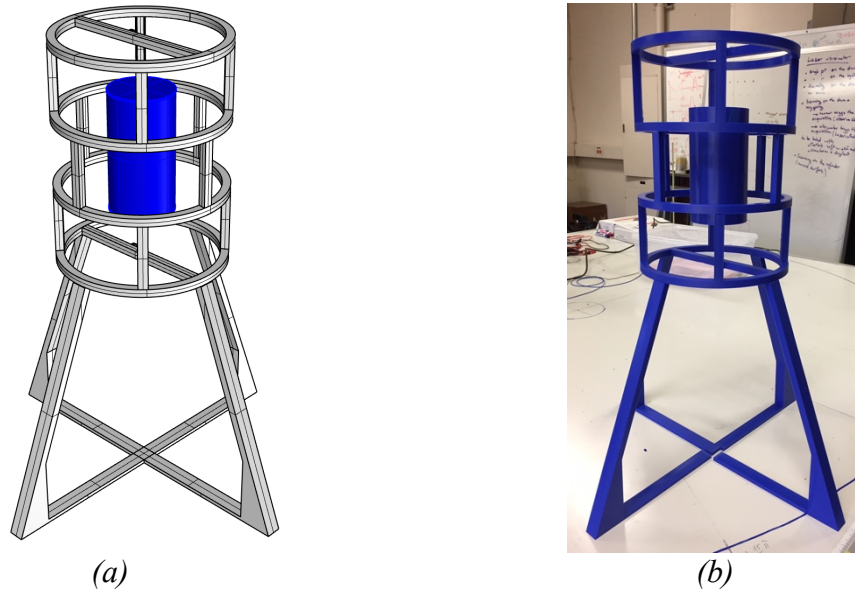


Figure 6: (a) 3D model depicting test target (inner blue/dark cylinder) and supporting sensor scaffold (outer white/light structure) to which the MEMS PCB units will be attached.  
(b) Actual scaffold and target constructed in a large form-factor 3D printer.

The sensors themselves are custom designed Printed Circuit Board (PCB) units (Fig. 7), utilizing pairs of digital MEMS microphones and complimentary logic for reliable data transmission over Low Voltage Differential Signalling (LVDS). The microphones are self-contained systems, providing signal conditioning, an analog-to-digital converter, decimation and anti-aliasing filters, and power management, all in a very small integrated package (4mm x 3mm x 1mm) capable of sampling rates up to 48kHz. This eliminates the need for any analog logic in the external data acquisition (DAQ) system, greatly reducing the cost and complexity, with the additional benefit of reduced susceptibility to noise since all sampling/conversions occur at the sensor end-point.

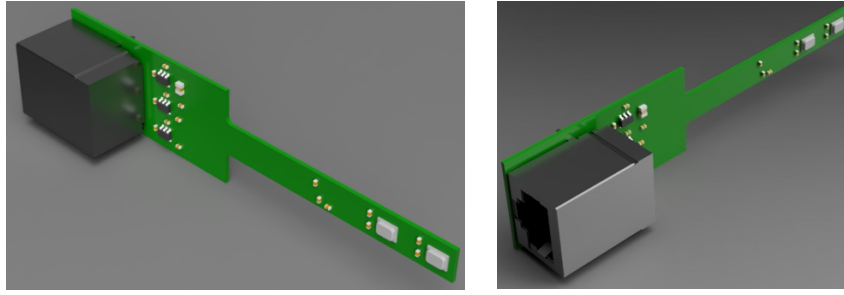


Figure 7: 3D renderings of the dual MEMS microphone PCB, ~10cm L x 2cm W. Signals are transmitted via LVDS over standard CAT-6 cabling

The DAQ unit driving these sensors is now only responsible for handling the streams of binary data coming from the microphones, and providing the (also digital) sampling and base clock signals to them. This can be accomplished through logic defined on a Field Programmable Gate Array (FPGA) system, and is currently working with a small device capable of supporting up to 32 microphone pairs. Scaling the system out is accomplished by either adding more FPGA interfaces in parallel, or moving up to larger FPGA devices, with support for up to 128 dual-mic boards each. An optional multiplexing serializer/de-serializer (SerDes) can be interposed between the microphones and the FPGAs to reduce the number of wires required while also increasing data transmission distances.

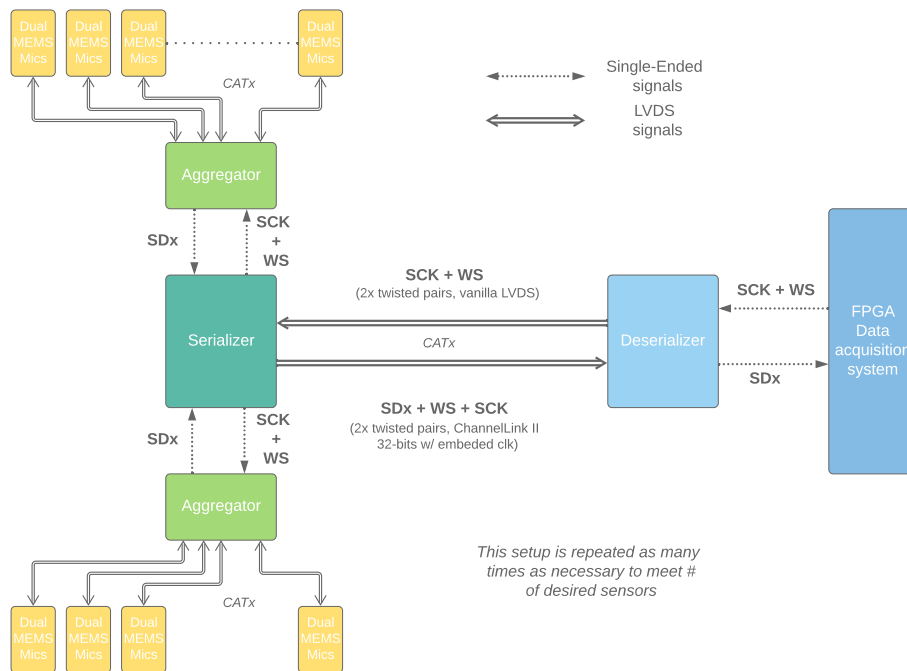
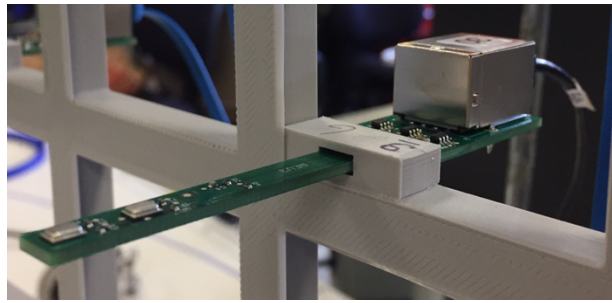


Figure 8: Schematic overview of full acoustic array acquisition system with optional SerDes interposer for extending data transmission distances and compressing the number of required wires/cables

To check the validity of the experimental set-up, a preliminary experiment using 10 pairs of digital MEMS microphones as the one shown on Figure 9 is first implemented to measure the response of a plastic capped pipe with a thickness  $d=2.5$  mm, an outer radius  $r=40$ mm and a height  $h=150$ mm.





*Figure 9: Zoom of the mounting system for holding the PCB that contains the MEMS microphones*

As shown on Fig. 6, this target is embodied inside the scaffold that holds the PCBs containing the MEMS sensors (Fig. 8). Both structures, target and scaffold, are 3D printed using PLA plastic that has a density  $\rho = 1250 \text{ kg/m}^3$ , a Young modulus  $E = 3.5 \text{ GPa}$  and a Poisson ratio  $\nu = 0.33$ . Each PCB points toward the axis of the capped cylinder that is centred with the scaffold axis. The MEMS microphones are respectively located 5 mm and 15 mm off the target surface. Measurements are conducted by uniformly moving a white noise source around the {source + scaffold} in order to extract the capped pipe response (structural admittance/impedance) around its  $n = 2$  mode following the approach described in section 2. According to numerical and analytical simulations, this mode occurs at 960.83 Hz (Figure 10) for the studied capped pipe when filled with air.

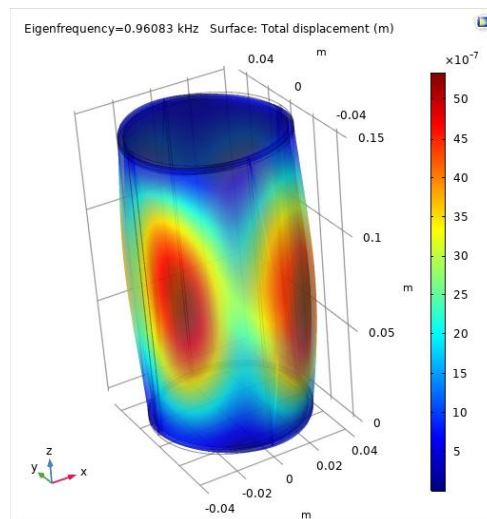


*Figure 10: Mode  $n=2$  of the capped pipe filled with air.*

Once these preliminary tests are performed and validated, the next measurements will aim at estimating low and higher modes of the in-vacuo response of a complex shape target such as an unexploded ordnance. To do so, measurements will be performed with a larger array made of 250 MEMS microphone pairs like the one shown on **Error! Reference source not found.** Figure 9.

## ACKNOWLEDGEMENTS

This research is supported by the U.S. Office of Naval Research.

## REFERENCES

- [1] Yu. I. Bobrovnskii, Impedance theory of sound scattering: General relations, *Acoust. Phys.*, 52(5), 2006, 513-517.
- [2] S. T. Rakotonarivo, W. A. Kuperman and Earl G. Williams, Prediction of a body's structure impedance and scattering properties using correlation of random noise, *J. Acoust. Soc. Am.* 134(6), 2013, 4401-4411.
- [3] I. Lucifredi and H. Schmidt, Subcritical scattering from buried elastic shells, *J. Acoust. Soc. Am.* 120(6), 2006, 3566-3583.
- [4] G. V. Borgiotti, Effect of the compliance on the scattering of an elastic object immersed in fluid: A general formulation, *J. Acoust. Soc. Am.* 87(3), 1990, 1055-1061.
- [5] C. F. Gaumond and T. Yoder, Determination of structural impedance from scattering data, *J. Acoust. Soc. Am.* 93(3), 1995, 1415-1422.
- [6] Earl G. Williams, Jeffery D. Tippmann, Sandrine T. Rakotonarivo, Zachary J. Waters, Philippe Roux and W. A. Kuperman, Experimental estimation of in vacuo structural admittance using random sources in a non-anechoic room, *J. Acoust. Soc. Am.* 142, 2017, 103-109.
- [7] Earl G. Williams, *Fourier Acoustics*, Academic Press, London, 1999.
- [8] W. A. Veronesi and J. D. Maynard. Digital holographic reconstruction of sources with arbitrarily shaped surfaces. *J. Acoust. Soc. Am.*, 85:588–598, 1989.
- [9] N. Valdivia and E. Williams, Study of the comparison of the methods of equivalent sources and boundary element methods for near-field acoustic holography, *J. Acoust. Soc. Am.* 120, 2006, 3694-3705.
- [10] Chuan-Xing Bi, Xin-Zhao Chen, and Jian Chen, Sound field separation technique based on equivalent source method and its application in nearfield acoustic holography, *J. Acoust. Soc. Am.* 123(3), 2008, 1472-1478.
- [11] Efren Fernandez-Grande, Finn Jacobsen and Quentin Leclerc, Sound field separation with sound pressure and particle velocity measurements, *J. Acoust. Soc. Am.* 132(6), 2012, 3818-3825.
- [12] E. G. Williams, the nearfield acoustical holography (NAH) experimental method applied to vibration and radiation in light and heavy fluids, *Computers & Structures*, Vol 65, No. 3, pp 323-335, 1997.